Journal of Industrial and Systems Engineering
Vol. 12, Special issue on Statistical Processes and Statistical Modeling, pp. 15-34
Winter (January) 2019

New phase II control chart for monitoring ordinal contingency table based processes

Ahmad Hakimi[1], Hiwa Farughi[1*], Amirhossein Amiri[2], Jamal Arkat[1]

[1]*Department of Industrial Engineering, Faculty of Engineering, University of Kurdistan, Sanandaj, Iran*
[2]*Department of Industrial Engineering, Faculty of Engineering, Shahed University, Tehran, Iran*

a.hakimi@eng.uok.ac.ir , h.farughi@uok.ac.ir , amiri@shahed.ac.ir, j.arkat@uok.ac.ir

Abstract

In some statistical process monitoring applications, quality of a process or product is described by more than one ordinal factor called ordinal multivariate process. To show the relationship between these factors, an ordinal contingency table is used and modeled with ordinal log-linear model. In this paper, a new control charts based on ordinal-normal statistic is developed to monitor the ordinal log-linear model based processes in Phase II. Performance of the proposed control chart is evaluated through simulation studies and a real numerical example. In addition, to show the efficiency of ordinal-normal control chart, performance of the proposed control chart is compared with an existing Generalized-*p* chart. Results show the better performance of the proposed control chart in detecting the out-of-control condition.

Keywords: Statistical process monitoring, ordinal contingency table, ordinal-normal control chart, Phase II

1- Introduction

Statistical process monitoring (SPM) has been widely used to monitor various industrial processes with multiple correlated quality characteristics following some distributions including binomial/multinomial, Poisson, Gamma and so on. Some processes known as multivariate ordinal involve more than one quality characteristics, for which multivariate control charts based on multivariate generalized linear models (MGLMs) are used for monitoring purpose. MGLMs use link functions including nominal log-linear model (NMLLM) and ordinal log-linear model (OLLM) to relate the mean of a multivariate categorical quality characteristic to some predictor variables (or factors). Some researchers used ordinal contingency tables in real applications. For example, Armitage (1995) used two-way ordinal contingency table from a randomized study to compare two treatment groups (including A and B categories) for a gastric ulcer crater.

*Corresponding author
ISSN: 1735-8272,

The change in the size of the ulcer crater variable is also including four categories as larger, less than 2/3 Healed, 2/3 or more Healed and Healed. Another research is 2006 general social survey. Respondents were asked, "Taken all together, would you say that you are very happy, pretty happy, or not too happy?" Also, they are asked regarding family income with question "Compared with American families in general, would you say that your family income is below average, average, or above average?” Based on these two questions, the OCT is formed (Agresti 2010).

In SPM, the contingency table is the most widely used tool for simultaneous monitoring of multivariate categorical processes (Kamranrad et al. 2017a). In addition, to show the relationship between ordinal factors and corresponding observations in ordinal contingency table (OCT) cells, OLLM are used. For example, Subramanyam and Rao (1989) examined the independency hypothesis in $2 \times n$ OCT and calculated odds ratio for several conditions. Beh and Davy (1998) developed categorical Pearson chi-square for three-way contingency table under orthogonal multinomial distribution. Zafar et al. (2013) applied OLLM along with correspondence analysis in pharmaceutical industry to predict the Opiate material in drug detecting processes. Brzezińska (2016) proposed model for OCT by considering linear effect, rows, columns and simultaneous effects. Note that, there is no research in OLLM/OCT based processes monitoring in SPM and just, there are some researches presented to monitor multivariate nominal processes using a log-linear model. For example, Zhen and Basawa (2009) presented a model related to a time-dependent contingency table called the time series table with categorical data. Kieffer et al. (2012) used a generalized form of the contingency table proposed by Kijima and Matsui (2006) to evaluate genetic characteristic effects of 10,000 individuals on the occurrence of the cancer on nine parts of their bodies.

A new multivariate SPC procedure was developed by Zou and Tsung (2011) to monitor the shape parameters using exponentially weighted moving average (EWMA) control chart by adapting the spatial-sign covariance matrix. Moreover, Yashchin (2012) used the generalized likelihood ratio test to develop a control chart with categorical observations, where the parameters are subject to sudden and unpredictable changes at unknown time points. In addition, he discussed about parameter estimation for categorical data in the presence of sudden changes. His proposed methodology was used to monitor a semiconductor production system. Li et al. (2012) proposed a generalized likelihood ratio test (GLRT) for Phase II monitoring of multivariate categorical processes based on the binomial and multivariate multinomial distribution using the log-linear model. They presented the EWMA-GLRT to improve the performance of the GLRT control chart under small shifts in parameters of the log-linear model. Li et al. (2013) proposed a new multivariate nonparametric statistical process control chart to monitor the shape parameters by integrating a multivariate spatial-sign test and EWMA scheme. A new multivariate binomial/multinomial control chart was presented by Li et al. (2014a) to monitor multivariate categorical processes where there is correlation between categorical quality characteristics. They used a log-linear model to illustrate the relationship among categorical variables that are compatible with multivariate binomial/multinomial distributions. It was shown that their proposed control chart is robust to detect different shifts in Phase II. After that, Kamranrad et al. (2017a) proposed GLT and EWMA-GLT schemes to monitor the multivariate categorical processes in Phase II. In addition, they proposed new diagnostic scheme to diagnose the parameter(s) responsible for out-of-control conditions based on GLT and EWMA-GLT in Phase II. Kamranrad et al. (2017b) proposed Wald and Stuart score test statistics for Phase II monitoring of the nominal contingency tables. To improve the performance of proposed control charts in small and moderate shifts in the contingency table parameters, they proposed EWMA-Wald and EWMA-Stuart score test statistics. In addition, they presented new schemes to diagnose the cell(s) responsible for out-of-control condition. Results showed the superiority of EWMA-Wald control chart rather than the other proposed charts in small, moderate and large shifts in NLLM slope parameters. Note that Kamranrad et al. (2017a and 2017b) considered contingency tables with multivariate nominal processes while this research concentrates on the multivariate ordinal processes. Nominal variables have two or more categories without having any kind of natural order while an ordinal variable is a categorical variable for which the possible values are ordered.

For monitoring ordinal categorical process, Li et al. (2014b) proposed an ordinal-normal control chart to detect location changes in univariate ordinal processes. In other words, they presented new control chart to monitor the ordinal logistic regression based processes in phase II. Hakimi et al. (2018) proposed two control charts including multivariate ordinal categorical and multivariate Generalized-*p* to monitor the OLLM processes in phase II. For the sake of improvement in detecting shifts in the parameters of OLLM, this paper develops a control chart based on ordinal-nominal (O-N) statistic to monitor the ordinal contingency table (OCT) based processes in phase II.

The rest of this paper is as follows: in the next section, the OCT based processes and related models (i.e. OLLM) along with their parameters are defined. The proposed statistic and the control limits for monitoring OLLM in Phase II are discussed in section 3. The performance of the proposed control charts is evaluated using simulation studies in section 4. In addition, a numerical example is applied in section 5 to evaluate the efficiency of the proposed control chart. Finally, concluding remarks and future research are given in section 6.

2- The multivariate ordinal processes

The multivariate ordinal processes have at least two factors with two or more ordered levels represented by OCT. The most widely used model to analyze OCT is the OLLM. The OLLM effectively characterizes the association and interaction effects among the ordinal variables and therefore it can be used to develop multivariate ordinal control charts.

2-1- The ordinal log-linear model

As mentioned before, the OCT is used to show the simultaneous relationship between two or more ordinal factors. Suppose there are p variables such as $y_1, y_2, ..., y_p$ each with h_i , $i = 1, 2, ..., p$ possible levels. Therefore, the cells of the table represent $h_1 \times h_2 \times ... \times h_p$ possible outcomes (Kamranrad et al. 2017a). In order to model the relationship between the count in each cell and the ordinal variable levels associated with it, the OLLM has been developed in the literature. Suppose a contingency table with two ordinal factors (y_1, y_2) with h_1 and h_2 categories. Now, the OLLM is defined as

$$\log \mu_{ij} = \mu + \alpha_i + \beta_j + \varphi(u_i - \bar{u})(v_j - \bar{v}), \tag{1}$$

where, $\mu_{ij} = N\pi_{ij}$ is the expected observation value for cell (*i*,*j*). u_i and v_j are the row and column scores, respectively such that $u_i = i$ and $v_j = j$. In addition, μ is the constant effect, α_i and β_j are the main effects of the *i*th row and *j*th column, respectively. Note that, φ is defined as linear by linear interaction parameter in OLLM which can be estimated by the following equation:

$$\log\left(\frac{\mu_{ij}\ \mu_{i+1.j+1}}{\mu_{i.j+1}\mu_{i+1.j}}\right) = \varphi(u_i - u_{i+1})(v_j - v_{j+1}), \tag{2}$$

where, $(u_i - u_{i+1}) = 1$ and $(v_j - v_{j+1}) = 1$. It is noted that, in Phase-I monitoring of OLLM (according to unknown parameters), parameters could be estimated using iterative Newton's single-dimensional algorithm (Zafar et al. 2013).

Based on the log-linear model for nominal factors (Kamranrad et al. 2017a), the OLLM for two factors is defined as:

$$\log \boldsymbol{\mu} = \beta_0 + \beta_1 y_1 + \beta_2 y_2 + \varphi(y_1 - \bar{y}_1)(y_2 - \bar{y}_2). \tag{3}$$

where, $\boldsymbol{\mu}$ is the expected counts vector for OCT and $\bar{y}_i$ ($i = 1, 2$) is the mean of the ith ordinal factor.

2-2- The generalized ordinal log-linear model

Equation (3) can be extended for p factors as follows:

$$\begin{aligned}\log \boldsymbol{\mu} &= \beta_0 + \beta_1 y_1 + \beta_2 y_2 + \ldots + \beta_p y_p + \varphi_{12}(y_1 - \bar{y}_1)(y_2 - \bar{y}_2) + \ldots + \varphi_{1p}(y_1 - \bar{y}_1)(y_p - \bar{y}_p) + \ldots \\ &+ \varphi_{2p}(y_2 - \bar{y}_2)(y_p - \bar{y}_p) + \ldots + \varphi_{p-1,p}(y_{p-1} - \bar{y}_{p-1})(y_p - \bar{y}_p) + \varphi_{123}(y_1 - \bar{y}_1)(y_2 - \bar{y}_2)(y_3 - \bar{y}_3) + \ldots \\ &+ \varphi_{p-2,p-1,p}(y_{p-2} - \bar{y}_{p-2})(y_{p-1} - \bar{y}_{p-1})(y_p - \bar{y}_p) + \ldots + \varphi_{1,\ldots,p-1,p}(y_1 - \bar{y}_1)\ldots(y_{p-1} - \bar{y}_{p-1})(y_p - \bar{y}_p)\end{aligned} \tag{4}$$

where, $\boldsymbol{\mu}$ is the expected counts vector for OCT and $\bar{y}_i$ ($i = 1, 2, \ldots, p$) is the mean of the ith ordinal factor.

Note that, Li et al. (2014b) proposed the univariate ordinal-normal control chart in Phase II which is the base statistic for our research. Hence, in this section we overview this control chart as follows:

2-3- An overview of the univariate ordinal-normal control chart

Li et al. (2014b) proposed ordinal-normal control chart to monitor the univariate ordinal based processes in Phase II. Suppose that there are known IC probabilities $p_k^{(0)}$ (k=1,2,…,h) for each ordinal level of the categorical factor. Hence, the known cumulative probabilities are $c_k = \sum_{j=1}^{k} p_k^{(0)}$ (k=0,1,2,…,h).
In particular, given the thresholds a_k (k=1,2,…,h), the probabilities p_k (k=1,2,…,h) corresponding to h ordinal levels of the categorical factor can be obtained by $p_k = F(a_k) - F(a_{k-1})$.

Suppose that, there are h ordinal levels for a categorical factor. Hence, there are also h class intervals covering the values of the continuous variable that determines the factors. Such intervals are formed by some thresholds a_k (k=1,2,…,h)

$$-\infty = a_0 < a_1 < \ldots < a_{h-1} < a_h = \infty \ .$$

The corresponding statistic (S_i) for ordinal-normal control chart is presented as follows:

$$S_i = \left| \sum_{k=1}^{h} \frac{1}{p_k^{(0)}} \left[\phi\left(\Phi^{-1}\left(c_{k-1}^{(0)}\right)\right) - \phi\left(\Phi^{-1}\left(c_k^{(0)}\right)\right) \right] z_{ik} \right|, \tag{5}$$

where, ϕ and Φ are the probability distribution function (pdf) and cumulative distribution function (cdf) of the standard normal distribution with mean (μ) equals to 0 and variance (σ) equals to 1, respectively. Note that, the pdf and cdf of the combined logistic-normal distribution are defined as follows, respectively:

$$f(x) = \frac{e^{-(x-\mu)/\sigma}}{\sigma(1 + e^{-(x-\mu)/\sigma})^2} \ \textit{and} \ F(x) = \frac{1}{1 + e^{-(x-\mu)/\sigma}} \ .$$

In addition, z_i can be calculated as the following equation:

$$\mathbf{z}_i = b_{0,i,\lambda}^{-1} \sum_{j=1}^{i} (1-\lambda)^{i-j} \mathbf{n}_j \ , \tag{6}$$

where, $\mathbf{n}_i = [n_{i1}, \ldots, n_{ih}]^T$ is the ith ordinal level count vector of size N which is subject to multinomial distribution $MN(N, \mathbf{p}^{(0)})$ with in-control $\mathbf{p} = [p_1^{(0)}, \ldots, p_h^{(0)}]^T$ the ordinal level count n_k (k=1,2,…,h) with total count as $N=\sum_{j=1}^{h} n_k$ which follows $MN(N,\mathbf{p})$, where $\mathbf{p}=[p_1,...,p_h]^T$. Moreover, the $b_{0,i,\lambda}^{-1}$ is a sequence of constants put in place to ensure that all the weights sum up to 1 calculated by equation (7) and $0<\lambda<1$ is the smoothing parameter and $\mathbf{z}_i=\left[z_{i1},z_{i2},...,z_{ih}\right]$.

$$b_{t_0,t_1,\lambda}^{-1}=\sum_{j=t_0+1}^{t_1}(1-\lambda)^{t_1-j} \tag{7}$$

The statistic rejects the null hypothesis, if R_i is larger than a specified threshold determined by simulation to obtain a desired in-control average run length (ARL_0). Note that, the S_i scheme is used to test the following hypothesis:

$$\begin{aligned}&\mathbf{H}_0:\delta=0\\&\mathbf{H}_1:\delta\neq 0\end{aligned},$$

where δ is the unknown location shift in ordinal based process parameters. Interested readers are referred to (Li et al. 2014b) for more details.

As mentioned, in this paper, performance of the proposed control chart is compared with an existing multivariate Generalize-*p* control chart by Hakimi et al. (2018). Hence, in this paper we overview this control chart as follows.

2-4- An overview of the multivariate Generalize-p control chart

Hakimi et al. (2018) proposed Generalized-*p* control chart to monitor the multivariate ordinal processes in Phase II. Suppose *p* ordinal factors with h_1, h_2,…, h_p levels. Hence, the modified EWMA/MG-*p* charting statistic (MG_t) is developed as follows:

$$MG_t=\frac{1}{N}(\mathbf{w}_t-N\mathbf{q}^{(0)})^T\boldsymbol{\Sigma}^{-1}(\mathbf{w}_t-N\mathbf{q}^{(0)}), \tag{8}$$

where, $N=\sum_{i=1}^{h_1}\sum_{j=1}^{h_2}\sum_{k=1}^{h_3}...\sum_{p=1}^{h_p}f(i,j,k,...,p)$ is the total sample size and $\mathbf{w}_t=[z_{t111...1}^{(0)},z_{t112...1}^{(0)},z_{t11h_3...h_p}^{(0)},...,z_{t(h_1-1)(h_2-1)(h_3-1)...(h_p-1)}^{(0)}]^T$. In addition, covariance matrix for EWMA/MG-*p* is defined as follows:

$$\boldsymbol{\Sigma}=\begin{bmatrix}\boldsymbol{\Sigma}_{h_1} & \boldsymbol{\Sigma}_{h_1h_2} & \boldsymbol{\Sigma}_{h_1h_3} & \cdots & \boldsymbol{\Sigma}_{h_1h_p}\\ \boldsymbol{\Sigma}_{h_1h_2} & \boldsymbol{\Sigma}_{h_2} & \boldsymbol{\Sigma}_{h_2h_3} & \cdots & \boldsymbol{\Sigma}_{h_2h_p}\\ \boldsymbol{\Sigma}_{h_1h_3} & \boldsymbol{\Sigma}_{h_2h_3} & \boldsymbol{\Sigma}_{h_3} & \cdots & \boldsymbol{\Sigma}_{h_3h_p}\\ \vdots & \vdots & \vdots & \ddots & \vdots\\ \boldsymbol{\Sigma}_{h_1hp} & \boldsymbol{\Sigma}_{h_2h_p} & \boldsymbol{\Sigma}_{h_3h_p} & \cdots & \boldsymbol{\Sigma}_{h_p}\end{bmatrix} \tag{9}$$

where, $\mathbf{\Sigma}_{h_i h_j}$ is the (h_i-1)×(h_j-1) matrix, which is the covariance matrix between levels of the factors *i* and *j*. At any specific monitoring time, if $MG_t>S$, the null hypothesis is rejected, i.e., the process is out-of-control, where *S* is set to obtain a desired in-control average run length (ARL_0).

3- Proposed method

Consider *p*-way OCT (*p*-ordinal factors) each with h_1, h_2,…, h_p categories. Now, the proposed multivariate ordinal-normal statistic (*MONS*) is developed as follows.

$$MONS_t = \left| \sum_{i=1}^{h_1} \sum_{j=1}^{h_2} \sum_{k=1}^{h_3} \dots \sum_{p=1}^{h_p} \frac{1}{P_{i\,jk\dots p}^{(0)}} \left[f\left(F^{-1}\left(c_{i\,jk\dots p-1}^{(0)}\right)\right) - f\left(F^{-1}\left(c_{i\,jk\dots p}^{(0)}\right)\right) \right] z_{ijk\dots p} \right|, \tag{10}$$

where, $P_{i\,jk\dots p}^{(0)} = F(a_{i\,jk\dots p}) - F(a_{i\,jk\dots p-1})$ such that, intervals are formed by some thresholds $a_{i\,jk\dots p}$ ($i=1,\dots h_1,\ j=1,\dots,h_2, k=1,\dots,h_3,\dots,\ p=1,\dots,h_p$) for each cell of OCT. In addition, *f* and *F* are the pdf and cdf of the standard normal distribution, respectively and $c_{i\,jk\dots p}^{(0)}$ is the in-control cumulative probability calculated from the following equation:

$$c_{i\,jk\dots p}^{(0)} = \sum_{i=1}^{h_1} \sum_{j=1}^{h_2} \sum_{k=1}^{h_3} \dots \sum_{p=1}^{h_p} \pi_{ijk\dots p}^{(0)}\ , \tag{11}$$

where, $\pi_{ijk\dots p}^{(0)} = \dfrac{n(i,\,j,k,\dots,\,p)}{\sum_{i=1}^{h_1} \sum_{j=1}^{h_2} \sum_{k=1}^{h_3} \dots \sum_{p=1}^{h_p} n(i,\,j,k,\dots,\,p)}$ is the in-control probability for the ordinal (*i*, *j*, *k*,…,*p*) cell count and $n(i,\,j,k,\dots,\,p)$ is the ordinal level count for cell (*i*,*j*,*k*,…,*p*). Furthermore, $\mathbf{z}_t$ is:

$$\mathbf{z}_t = b_{0,t,\lambda}^{-1} \sum_{s=1}^{t} (1-\lambda)^{t-s} \mathbf{n}_t\,, \tag{12}$$

where, $a_{t_1,t_2,\lambda}^{-1} = \sum_{t=t_1+1}^{t_2} (1-\lambda)^{t_2-t_1}$ and $\mathbf{n}_t = [n_{111\dots1t}\ n_{112\dots1t} \dots n_{11h_3\dots h_p t}\ n_{121\dots1t} \dots n_{12h_3\dots h_p t} \dots n_{h_1h_2 1\dots1t} \dots n_{h_1h_2h_3\dots h_p t}]$. At any specific monitoring time, if $MONS_t>L$, the null hypothesis is rejected, i.e. , the process is out-of-control, where *L* is set to obtain a desired in-control average run length (ARL_0).

4- Performance evaluation

The performance of the proposed control chart in terms of the out-of-control *ARL* $\left(ARL_1\right)$ criterion is first evaluated in this section. Then, a sensitivity analysis is performed on the size of the rows and the columns of the contingency table. In this study, contingency tables with 4 rows and with 5 columns are investigated. Meanwhile, a sensitivity analysis on the simultaneous increasing of rows and columns is performed.

4-1- Performance evaluation of the proposed control chart

In this subsection, simulation experiments are performed to evaluate the performance of the proposed MONS control chart in terms of ARL_1 under different shifts in the parameters of the OLLM in units of their corresponding standard deviations. In addition, to show the efficiency of the proposed control chart, performance of MONS is compared with an existing MG-*p* (Hakimi et al. 2018) control chart.

Consider a two-way contingency table with 3 rows and 4 columns. Note that, the UCLs of the MONS and MG-*p* charts based on 3×4 contingency table are set equal to 107.61and 0.93, respectively to obtain a desired in-control *ARL* of 200. Then, the ARL_1 values of the two mentioned control charts under different shifts in OLLM parameters and different smoothing parameters based on 5,000 simulation experiments are calculated and reported in Tables 1-4. Also, the standard error of the average run lengths (SEARL) are reported in the parenthesis below the *ARL* values. Moreover, the in-control parameter vector of the OLLM based on the mentioned contingency table is assumed $\boldsymbol{\beta}=\left[1,-0.5,\,-0.5,\,0.15\right]$. In addition, the in-control standard deviations of the OLLM parameters estimates are as follows:

$$\hat{\boldsymbol{\sigma}}_{0\hat{\boldsymbol{\beta}}}=[2.14,1.43,1.28,0.89],$$

Note that in this paper shifts will be imposed in the parameters of the OLLM in units of their corresponding standard deviations. The standard deviations of the parameters estimate in the OLLM are obtained by using the following covariance matrix:

$$\mathrm{cov}(\boldsymbol{\beta})=\{\mathbf{X}'[\mathbf{diag}(\boldsymbol{\mu})-\boldsymbol{\mu}\boldsymbol{\mu}'/N]\mathbf{X}\}^{-1}, \tag{13}$$

where $\mathbf{X}$ and $\boldsymbol{\mu}$ are the model matrix and the vector of the expected values of the contingency table cells, respectively. Also, $\mathbf{diag}(\boldsymbol{\mu})$ is a diagonal matrix of the values of the contingency table cells and *N* is the sample size of the contingency table (Agresti, 2002).

Table 1. The ARL and SEARL values under the different shifts in the intercept ($\beta_0+\gamma.\sigma_{\hat{\beta}_0}$)

λ	γ	-1.2	-0.8	-0.5	-0.2	-0.1	0	0.1	0.2	0.5	0.8	1.2
0.05	MONS	96.26 (1.05)	132.59 (1.67)	155.31 (1.94)	173.58 (2.00)	188.65 (2.04)	200.35 (2.69)	188.60 (2.21)	179.05 (2.01)	154.07 (1.68)	132.29 (1.35)	99.98 (1.05)
	MG-*p*	93.57 (1.13)	130.25 (1.95)	156.84 (1.99)	175.69 (2.04)	190.05 (2.11)	201.05 (3.32)	189.98 (2.05)	180.39 (2.02)	155.61 (2.00)	131.58 (1.97)	99.48 (1.01)
0.1	MONS	94.96 (1.06)	123.68 (1.49)	152.66 (1.79)	176.47 (1.99)	188.30 (2.02)	199.97 (2.69)	187.05 (2.00)	180.37 (1.93)	150.02 (1.21)	131.69 (1.14)	99.60 (1.00)
	MG-*p*	92.68 (1.27)	121.15 (1.90)	155.03 (1.97)	178.41 (2.01)	189.87 (2.14)	200.10 (3.05)	189.19 (2.10)	181.04 (2.06)	151.36 (1.84)	130.01 (2.00)	98.08 (1.05)
0.2	MONS	95.00 (1.02)	122.09 (1.36)	150.75 (1.65)	177.91 (1.97)	187.90 (2.25)	200.85 (2.09)	183.38 (2.00)	175.66 (1.99)	151.48 (1.64)	121.95 (1.59)	98.92 (1.08)
	MG-*p*	91.05 (1.70)	124.87 (1.95)	152.97 (1.87)	178.84 (1.94)	189.31 (1.99)	199.96 (2.68)	185.37 (1.95)	179.65 (1.92)	150.33 (2.01)	120.05 (2.01)	99.21 (1.06)

Table 2. The ARL and SEARL values under the different shifts in the first slope ($\beta_1 + \gamma.\sigma_{\hat{\beta}_1}$)

λ	γ	-1.2	-0.8	-0.5	-0.2	-0.1	0	0.1	0.2	0.5	0.8	1.2
0.05	MONS	1.00 (0.00)	9.25 (0.96)	26.10 (1.11)	113.28 (1.57)	179.60 (2.00)	200.05 (2.34)	177.62 (1.97)	115.05 (1.63)	27.79 (1.45)	8.40 (0.91)	1.00 (0.00)
	MG-p	1.00 (0.00)	6.92 (0.40)	26.29 (1.00)	116.49 (1.93)	183.67 (2.01)	201.30 (2.99)	180.69 (2.02)	116.39 (1.56)	26.75 (1.27)	7.63 (0.59)	1.00 (0.00)
0.1	MONS	1.00 (0.00)	7.95 (0.86)	24.15 (1.02)	110.54 (1.46)	178.12 (1.98)	200.29 (2.06)	175.66 (2.00)	115.68 (1.55)	25.04 (1.18)	7.69 (0.91)	1.00 (0.00)
	MG-p	1.00 (0.00)	6.74 (0.39)	23.05 (0.91)	110.63 (1.67)	182.35 (2.09)	200.18 (2.97)	183.54 (2.01)	119.67 (1.91)	25.97 (1.30)	6.35 (0.86)	1.00 (0.00)
0.2	MONS	1.00 (0.00)	5.69 (0.52)	26.53 (1.02)	100.30 (1.50)	176.19 (2.10)	199.56 (2.24)	172.21 (1.67)	108.34 (1.88)	23.14 (1.33)	6.50 (0.96)	1.00 (0.00)
	MG-p	1.00 (0.00)	3.89 (0.45)	28.41 (1.29)	100.14 (2.05)	180.25 (2.06)	200.04 (2.93)	181.02 (1.89)	109.54 (1.12)	25.20 (1.84)	3.92 (0.27)	1.00 (0.00)

Table 3. The ARL and SEARL values under the different shifts in the second slope ($\beta_2 + \gamma.\sigma_{\hat{\beta}_2}$)

λ	γ	-1.2	-0.8	-0.5	-0.2	-0.1	0	0.1	0.2	0.5	0.8	1.2
0.05	MONS	1.00 (0.00)	6.05 (0.91)	23.08 (1.00)	114.92 (1.48)	170.54 (1.94)	201.07 (2.14)	177.60 (2.00)	128.19 (1.69)	21.97 (0.99)	5.23 (0.47)	1.00 (0.00)
	MG-p	1.00 (0.00)	5.02 (0.31)	22.69 (0.92)	115.69 (1.25)	171.69 (2.02)	200.35 (2.98)	182.39 (2.09)	130.10 (2.00)	22.89 (0.91)	4.81 (0.19)	1.00 (0.00)
0.1	MONS	1.00 (0.00)	4.50 (0.29)	21.46 (0.81)	116.10 (1.43)	168.00 (1.88)	200.54 (2.67)	173.80 (1.98)	123.95 (1.80)	23.47 (1.01)	4.93 (0.49)	1.00 (0.00)
	MG-p	1.00 (0.00)	3.70 (0.21)	21.57 (0.89)	119.67 (1.09)	169.27 (2.01)	200.10 (3.01)	181.29 (2.11)	130.04 (1.69)	21.69 (0.98)	3.98 (0.32)	1.00 (0.00)
0.2	MONS	1.00 (0.00)	3.96 (0.33)	16.42 (0.93)	111.45 (1.25)	150.85 (1.77)	199.87 (2.51)	174.67 (2.00)	129.79 (1.91)	21.26 (1.11)	3.64 (0.47)	1.00 (0.00)
	MG-p	1.00 (0.00)	3.05 (0.88)	15.69 (0.98)	115.52 (1.00)	161.24 (1.89)	200.17 (2.99)	180.05 (2.09)	135.59 (2.00)	19.97 (1.30)	3.09 (0.29)	1.00 (0.00)

Table 4. The ARL and SEARL values under the different shifts in φ ($\varphi + \gamma.\sigma_{\hat{\varphi}}$)

λ	γ	-1.2	-0.8	-0.5	-0.2	-0.1	0	0.1	0.2	0.5	0.8	1.2
0.05	MONS	8.12 (0.90)	42.95 (1.00)	90.68 (1.35)	111.93 (1.66)	162.34 (1.94)	200.28 (2.49)	161.15 (2.02)	112.58 (1.61)	83.96 (1.49)	46.07 (1.37)	6.79 (0.38)
	MG-p	7.01 (0.39)	41.47 (0.82)	91.00 (1.80)	112.39 (1.91)	166.30 (2.05)	200.57 (2.99)	162.98 (2.02)	114.15 (1.99)	85.39 (1.53)	45.60 (0.99)	6.04 (0.30)
0.1	MONS	7.00 (0.34)	42.07 (1.09)	79.00 (1.32)	117.44 (1.83)	161.59 (1.97)	200.58 (2.75)	162.34 (1.65)	110.04 (1.58)	82.38 (1.29)	43.49 (1.14)	6.47 (0.31)
	MG-p	6.18 (0.52)	39.05 (0.92)	79.07 (1.69)	111.34 (1.87)	163.69 (2.02)	200.18 (3.14)	161.98 (2.00)	112.34 (1.79)	81.25 (1.78)	40.15 (1.05)	5.59 (0.19)
0.2	MONS	6.90 (0.67)	34.08 (0.97)	81.39 (1.52)	109.84 (1.66)	159.96 (1.94)	199.29 (2.03)	153.19 (1.63)	110.38 (1.57)	84.17 (1.13)	38.87 (1.39)	6.02 (0.36)
	MG-p	5.88 (0.17)	32.89 (1.01)	80.95 (2.04)	110.05 (1.64)	161.98 (2.05)	200.42 (2.90)	154.14 (1.75)	111.97 (1.78)	83.05 (1.36)	35.05 (1.41)	5.31 (0.21)

As it is clear from tables 1 to 4, the ARL_1 values of the MONS control chart are less than the ones obtained by the MG-*p* in small and moderate shifts in intercept and slope parameters of OLLM. Hence, the MONS chart has better performance compared to the MG-*p* in these mentioned shifts. MG-*p* has relatively better performance than the other control chart under large shifts in OLLM parameters. In addition, results show that the sensitivity of both control charts under shifts in the intercept is less than the other OLLM parameters. In addition, both control charts have better performance under shifts in the second slope parameter of the OLLM rather than the other parameters.

Furthermore, the performance of both control charts are compared based on different λ values and results show the better performance of the mentioned control charts under λ equals to 0.2. Note that, other simulation studies under different simultaneous shifts in the OLLM parameters based on λ=0.2 are done and some of them are reported in figures 1 to 6.

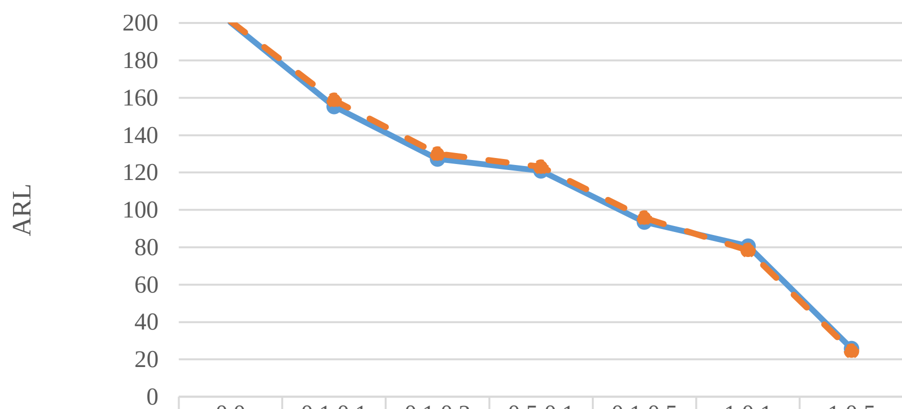

	0,0	0.1,0.1	0.1,0.2	0.5,0.1	0.1,0.5	1,0.1	1,0.5
MONS	200.36	155.3	127.19	120.97	93.58	80.66	25.94
MG-p	200.98	158.69	130.05	122.98	95.68	78.37	24.58

$\beta_0+\delta_0\sigma_{\beta 0}$, $\beta_1+\delta_1\sigma_{\beta 1}$

Fig 1. Performance comparison of the control charts for simultaneous shifts in the intercept and the first slope

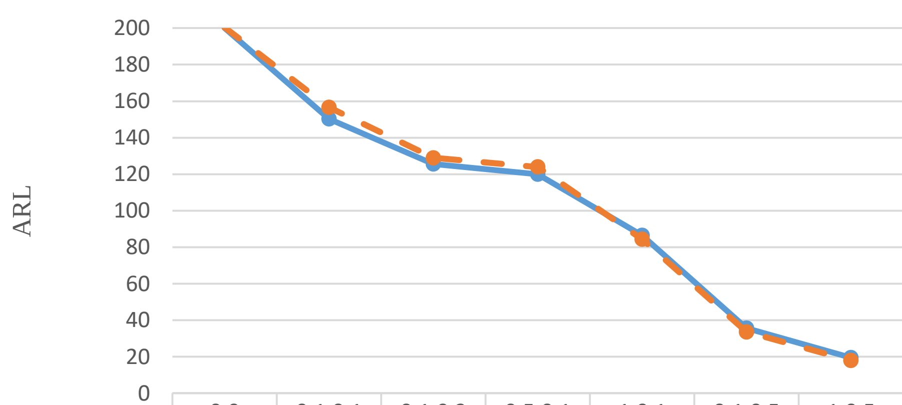

	0,0	0.1,0.1	0.1,0.2	0.5,0.1	1,0.1	0.1,0.5	1,0.5
MONS	200.09	150.33	125.64	119.96	86.45	35.64	19.47
MG-p	200.49	156.62	128.97	123.97	84.3	33.59	17.89

$\beta_0+\delta_0\sigma_{\beta 0}$, $\beta_2+\delta_2\sigma_{\beta 2}$

Fig 2. Performance comparison of the control charts for simultaneous shifts in the intercept and the second slope

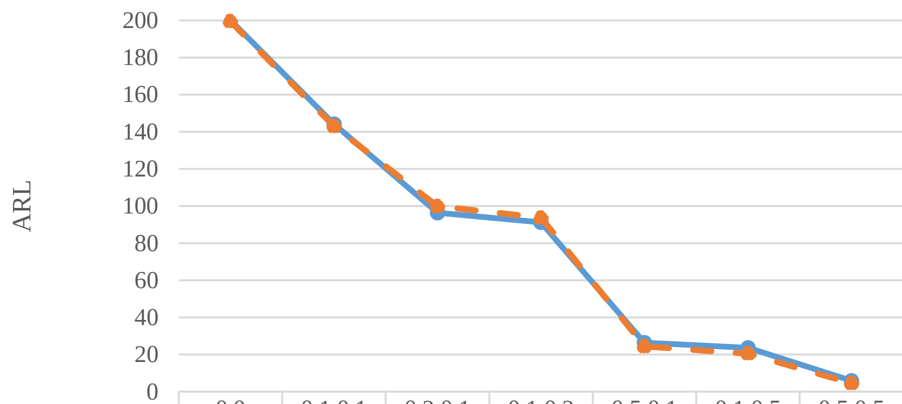

	0,0	0.1,0.1	0.2,0.1	0.1,0.2	0.5,0.1	0.1,0.5	0.5,0.5
MONS	200.05	144.04	96.39	91.26	26.44	23.62	6.02
MG-p	199.36	142.98	99.84	93.68	24.38	20.57	4.62

$\beta_1+\delta_1\sigma_{\beta 1}$, $\beta_2+\delta_2\sigma_{\beta 2}$

Fig 3. Performance comparison of the control charts for simultaneous shifts in the first and the second slope

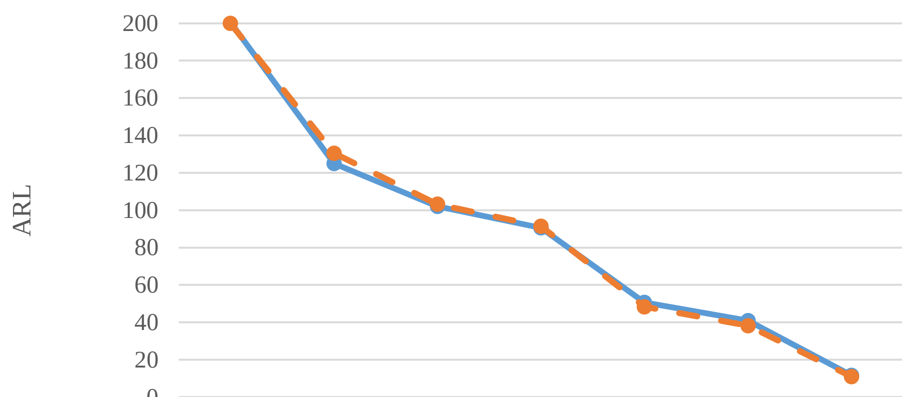

	0,0	0.1,0.05	0.5,0.05	0.1,0.1	1,0.05	0.1,0.2	0.5,0.2
MONS	200.59	124.98	101.97	90.56	50.68	40.94	11.66
MG-p	199.91	130.49	103.14	91.37	48.31	38.2	10.93

$\beta_0+\delta_0\sigma_{\beta 0}$, $\varphi+\delta_3\sigma_{\varphi}$

Fig 4. Performance comparison of the control charts for simultaneous shifts in the intercept and φ

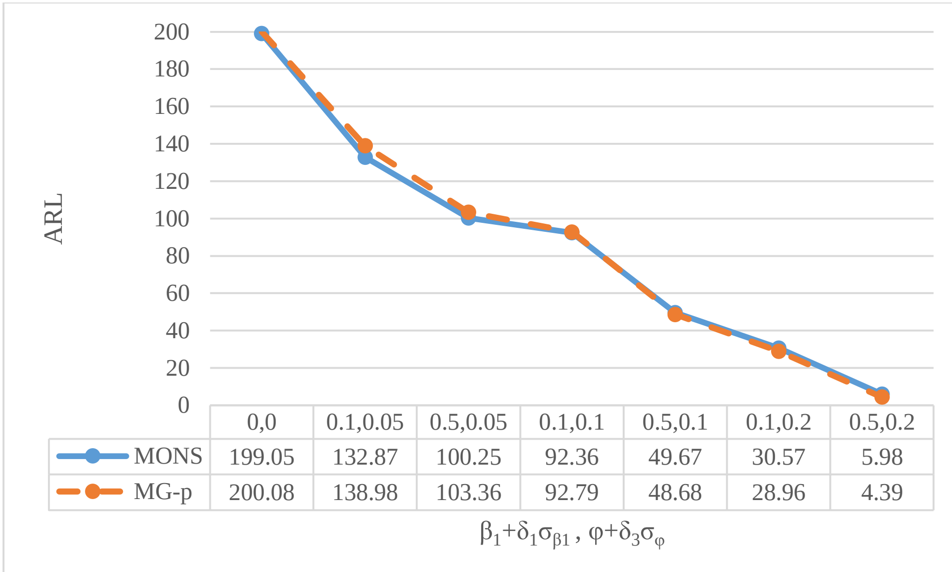

Fig 5. Performance comparison of the control charts for simultaneous shifts in the first slope and φ

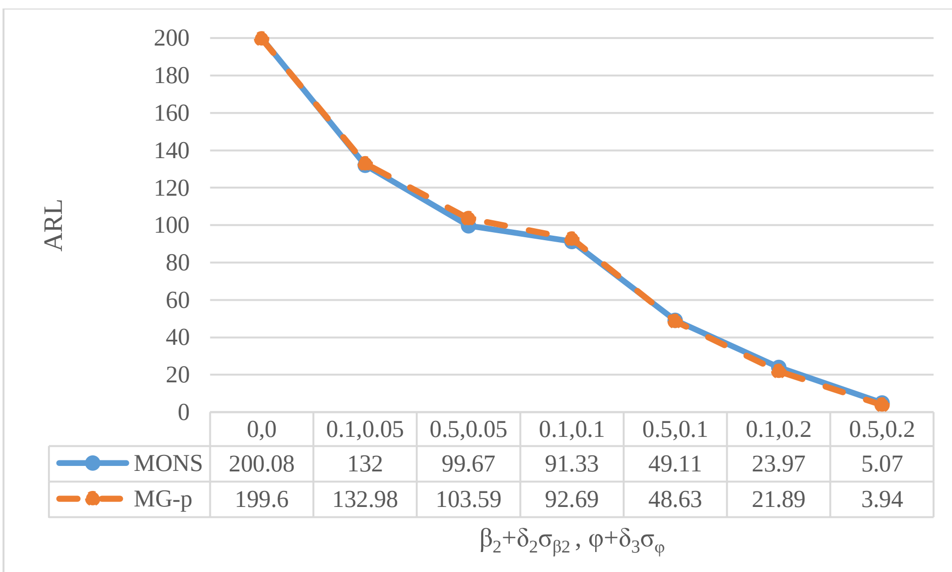

Fig 6. Performance comparison of the control charts for simultaneous shifts in the second slope and φ

As it is clear from figures 1-6, the simultaneous shifts in two slope parameters lead to better performance of the control charts under out-of-control conditions. These results are expected because the simultaneous effects of two shifts in log-linear model parameters are considered; hence the control charts should detect the out-of-control states more quickly. In addition, these figures also indicate that both control charts have better performance for different simultaneous shifts in both slope and φ rather than the other simultanous shifts in the OLLM parameters. Moreover, the results show that MONS control chart outperforms the MG-*p* control chart under small and moderate simaltaneous shifts in all the OLLM parameters.

In addition, a sensitivity analysis is performed on the size of the rows and the columns of the OCT. In this study, contingency tables with 4 rows and with 5 columns are investigated. Moreover, the performances of the proposed schemes are investigated under simultaneous increase in the size of rows and columns of the OCT. The results of the sensitivity analysis in terms of ARL_1 are summarized in tables 5 to 8.

Table 5. ARL and SEARL values of the proposed charts under different sizes of rows and columns for different shifts in the intercept ($\beta_0 + \gamma.\sigma_{\hat{\beta}_0}$)

Size	γ	-1.2	-0.8	-0.5	-0.2	-0.1	0	0.1	0.2	0.5	0.8	1.2
3×5	MONS	89.25 (1.13)	122.14 (1.61)	141.53 (1.80)	172.94 (2.02)	186.18 (2.35)	200.49 (2.88)	180.27 (2.17)	171.94 (2.93)	139.67 (1.86)	119.92 (1.66)	89.31 (1.45)
	MG-*p*	85.61 (1.04)	120.48 (1.69)	141.99 (2.00)	173.45 (2.21)	190.34 (2.68)	199.64 (2.99)	183.92 (2.58)	174.18 (2.00)	141.87 (2.01)	117.08 (1.87)	84.33 (1.21)
4×4	MONS	80.49 (1.17)	106.92 (1.39)	141.62 (1.66)	172.38 (1.93)	182.27 (2.08)	200.03 (2.63)	179.35 (2.17)	168.64 (2.00)	133.60 (1.90)	114.29 (1.46)	83.19 (1.25)
	MG-*p*	76.97 (1.61)	107.33 (1.34)	142.36 (1.61)	172.75 (2.12)	184.67 (2.37)	199.38 (3.00)	182.24 (2.24)	172.94 (2.30)	133.04 (1.90)	112.99 (1.41)	80.68 (1.39)
4×5	MONS	75.66 (1.32)	104.27 (1.55)	139.04 (1.69)	166.69 (2.00)	179.03 (2.02)	200.37 (2.28)	178.84 (2.38)	163.57 (2.01)	128.83 (1.69)	103.45 (1.62)	74.41 (1.39)
	MG-*p*	73.05 (1.08)	101.67 (1.42)	140.97 (1.49)	169.94 (2.43)	180.93 (3.05)	199.67 (2.97)	181.39 (2.59)	169.37 (2.00)	130.32 (1.90)	100.49 (1.31)	71.89 (1.00)

Table 6. ARL and SEARL values of the proposed charts under different sizes of rows and columns for different shifts in the first slope ($\beta_1 + \gamma.\sigma_{\hat{\beta}_1}$)

Size	γ	-1.2	-0.8	-0.5	-0.2	-0.1	0	0.1	0.2	0.5	0.8	1.2
3×5	MONS	1.00	7.99	26.08	114.45	177.81	201.02	176.69	112.48	26.61	8.13	1.00
		(0.00)	(0.90)	(0.98)	(1.33)	(2.00)	(2.63)	(2.03)	(1.73)	(1.06)	(0.93)	(0.00)
	MG-*p*	1.00	6.04	24.09	113.49	180.69	200.94	180.01	112.49	25.03	7.00	1.00
		(0.00)	(0.62)	(1.02)	(1.97)	(2.56)	(3.02)	(2.94)	(1.84)	(1.24)	(0.92)	(0.00)
4×4	MONS	1.00	8.09	27.75	111.49	176.05	200.31	174.36	110.08	25.98	8.18	1.00
		(0.00)	(0.88)	(1.00)	(1.21)	(1.81)	(2.30)	(2.01)	(1.59)	(1.00)	(0.82)	(0.00)
	MG-*p*	1.00	6.61	24.41	110.99	181.36	201.07	179.04	110.38	24.39	8.00	1.00
		(0.00)	(0.49)	(1.14)	(1.95)	(2.67)	(3.01)	(2.91)	(1.98)	(1.07)	(0.67)	(0.00)
4×5	MONS	1.00	7.91	27.00	110.62	175.63	200.58	170.96	108.37	25.61	8.05	1.00
		(0.00)	(0.84)	(0.98)	(1.46)	(2.00)	(2.67)	(1.95)	(1.93)	(1.04)	(0.65)	(0.00)
	MG-*p*	1.00	6.09	26.01	110.99	178.73	199.47	172.94	110.31	25.36	7.94	1.00
		(0.00)	(0.68)	(1.00)	(2.08)	(2.90)	(2.53)	(2.34)	(1.97)	(1.09)	(0.69)	(0.00)

Table 7. ARL and SEARL values of the proposed charts under different sizes of rows and columns for different shifts in the second slope ($\beta_2 + \gamma.\sigma_{\hat{\beta}_2}$)

Size	γ	-1.2	-0.8	-0.5	-0.2	-0.1	0	0.1	0.2	0.5	0.8	1.2
3×5	MONS	1.00 (0.00)	3.18 (0.22)	18.80 (0.67)	112.62 (1.51)	171.36 (2.07)	200.63 (2.45)	173.31 (2.02)	120.09 (2.03)	19.59 (0.68)	3.05 (0.28)	1.00 (0.00)
	MG-*p*	1.00 (0.00)	2.94 (0.23)	16.97 (0.69)	119.63 (1.92)	173.49 (2.09)	201.00 (3.05)	178.52 (2.96)	122.67 (1.97)	18.86 (0.96)	2.26 (0.20)	1.00 (0.00)
4×4	MONS	1.00 (0.00)	3.04 (0.29)	18.64 (0.58)	113.77 (1.52)	172.29 (2.31)	200.08 (2.47)	172.34 (2.32)	115.68 (2.15)	19.07 (0.78)	3.22 (0.30)	1.00 (0.00)
	MG-*p*	1.00 (0.00)	2.36 (0.12)	15.93 (0.49)	114.38 (1.56)	176.81 (2.69)	200.09 (2.68)	175.39 (2.28)	119.97 (2.00)	18.61 (0.97)	2.68 (0.27)	1.00 (0.00)
4×5	MONS	1.00 (0.00)	2.42 (0.17)	16.43 (0.29)	110.45 (1.63)	168.97 (2.50)	201.06 (2.05)	169.90 (2.04)	107.85 (1.63)	15.94 (0.33)	2.91 (0.13)	1.00 (0.00)
	MG-*p*	1.00 (0.00)	1.92 (0.08)	14.97 (0.19)	111.36 (1.80)	171.29 (2.15)	199.94 (2.97)	173.95 (2.63)	109.48 (1.69)	14.89 (0.26)	1.33 (0.09)	1.00 (0.00)

Table 8. ARL and SEARL values of the proposed charts under different size of rows and columns for different shifts in the φ ($\varphi + \gamma.\sigma_{\hat{\varphi}}$)

Size	γ	-1.2	-0.8	-0.5	-0.2	-0.1	0	0.1	0.2	0.5	0.8	1.2
3×5	MONS	5.01 (0.25)	32.96 (0.95)	80.52 (1.26)	106.47 (1.76)	153.39 (1.99)	200.38 (2.08)	151.64 (1.87)	106.09 (1.72)	80.35 (1.59)	32.98 (1.00)	4.05 (0.49)
	MG-*p*	4.08 (0.16)	31.97 (0.67)	79.67 (1.90)	108.06 (1.67)	155.07 (2.02)	200.01 (3.00)	153.98 (1.80)	108.25 (1.38)	82.64 (1.48)	32.05 (1.12)	3.14 (0.31)
4×4	MONS	4.55 (0.17)	29.65 (0.97)	77.46 (1.30)	104.98 (1.67)	151.27 (1.93)	200.97 (2.20)	152.67 (1.91)	105.32 (1.94)	78.96 (1.42)	32.47 (1.03)	3.92 (0.18)
	MG-*p*	3.00 (0.09)	27.74 (0.26)	79.93 (1.14)	105.68 (1.42)	154.19 (1.48)	200.94 (2.66)	155.30 (1.93)	108.89 (1.68)	80.06 (1.19)	30.57 (0.68)	2.84 (0.23)
4×5	MONS	3.31 (0.08)	26.92 (0.38)	74.93 (0.90)	102.94 (1.27)	150.08 (1.99)	199.75 (2.40)	149.93 (2.05)	102.39 (1.74)	75.52 (1.28)	29.68 (0.93)	2.67 (0.21)
	MG-*p*	1.69 (0.04)	23.50 (0.34)	72.26 (0.94)	104.50 (1.29)	154.00 (2.02)	200.53 (2.73)	153.34 (2.53)	105.60 (1.89)	75.49 (1.03)	27.04 (0.67)	2.00 (0.10)

As it is clear from tables 5 to 8, the MONS control chart has better performance compared to another proposed control chart in detecting out-of-control condition under small and moderate shifts in the parameters of the OLLM. In other words, the results in the mentioned tables indicate that the MONS control chart has better performance than the MG-*p* chart for monitoring the OCT based processes with 4 rows and 5 columns under small and moderate shifts. In addition, comparing the results between tables 1 to 4 and tables 5 to 8 show that by increasing the dimension of ordinal contingency table, the performance of both control charts improve in terms of both out-of-control *ARL* and *SEARL* criteria.

5- A numerical example

In this section, a numerical example is given to demonstrate the applicability of the proposed method and compare its performance with the existing method in monitoring OLLM based processes based on a real case extracted from Agresti (2010).

5-1- Performance comparison

Consider a real study by Lumley (1996) to compare an active treatment with a control treatment for patients having shoulder tip pain after laparoscopy surgery. The two treatments were randomly assigned to 41 patients. The patients rated their pain level on the fifth day after surgery. The OCT for this study is as following table:

Table 9. Shoulder tip score after laparoscopic surgery

Treatments	Pain score (1:low and 5:high)				
	1	2	3	4	5
Active	19	2	1	0	0
Control	7	3	4	3	2

In this subsection, we compare the performance of the proposed control chart and MG-*p* under two different shifts in the second slope and φ parameters of the OLLM. For this aim, we impose shifts of $-0.2\sigma_{\hat{\beta}_2}$ in β_2 and $0.2\sigma_{\hat{\varphi}}$ in φ, respectively and results are shown in Figures 7-10. The OLLM for the above OCT with two ordinal factors including treatment (T) and pain score (PS) under in-control state is defined as follows:

$$\log \boldsymbol{\mu} = 1 - 0.5T - 0.5PS + 0.15(T - \overline{T})(PS - \overline{PS});\ T = 1,2 \ \textit{and} \ PS = 1,2,3,4,5. \tag{14}$$

Note that, the UCLs of the MONS and MG-*p* charts based on the model in Equation (14) are set equal to 36.98 and 0.598, respectively by using 5000 simulation runs to achieve a desired in-control *ARL* of 200.

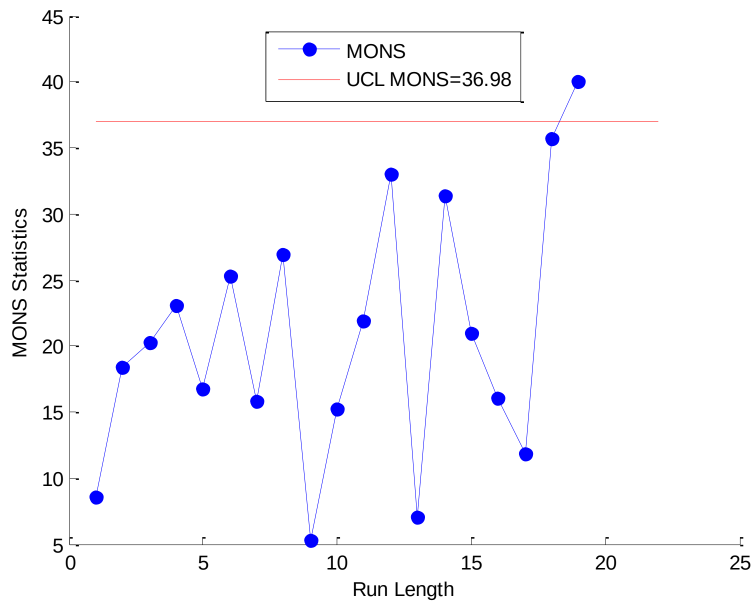

Fig 7. MONS control chart under -0.2 $\sigma_{\hat{\beta}_2}$ shift in β_2

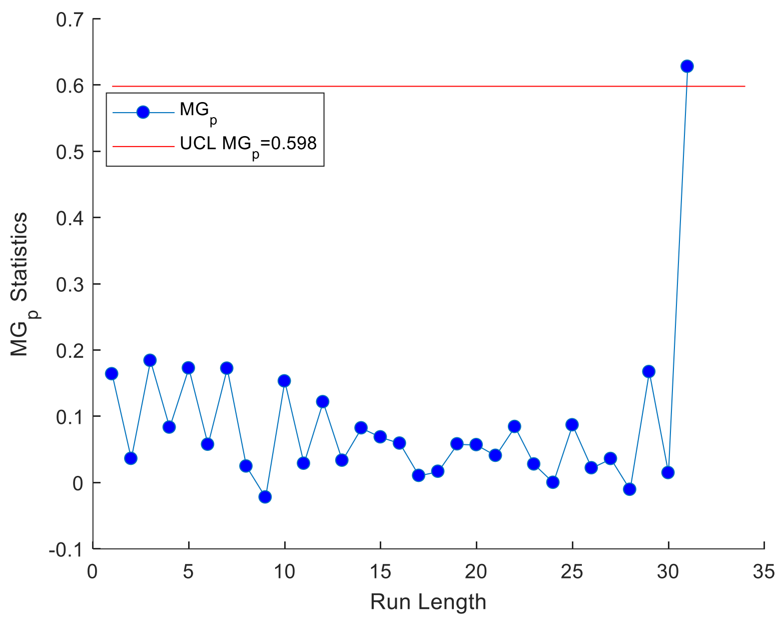

Fig 8. MG-*p* control chart under -0.2 $\sigma_{\hat{\beta}_2}$ shift in β_2

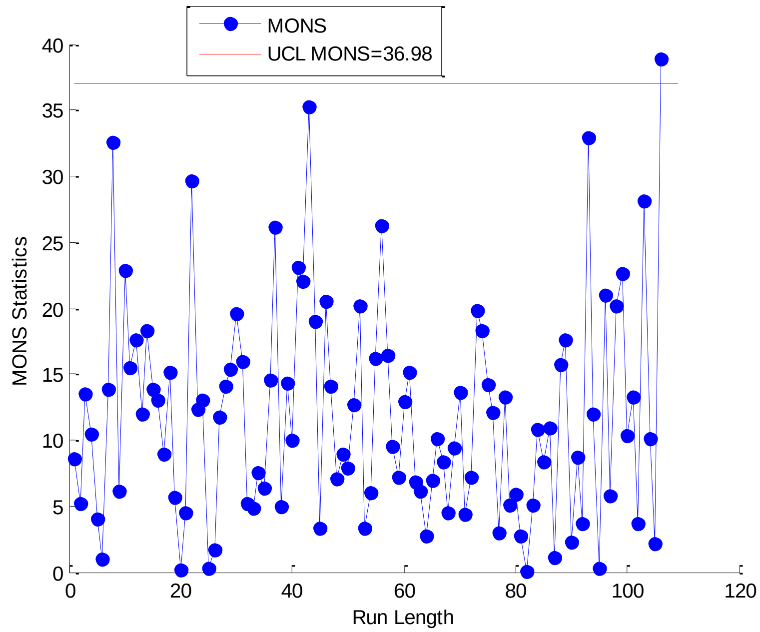

Fig 9. MONS control chart under 0.2 $\sigma_{\hat{\varphi}}$ shift in φ

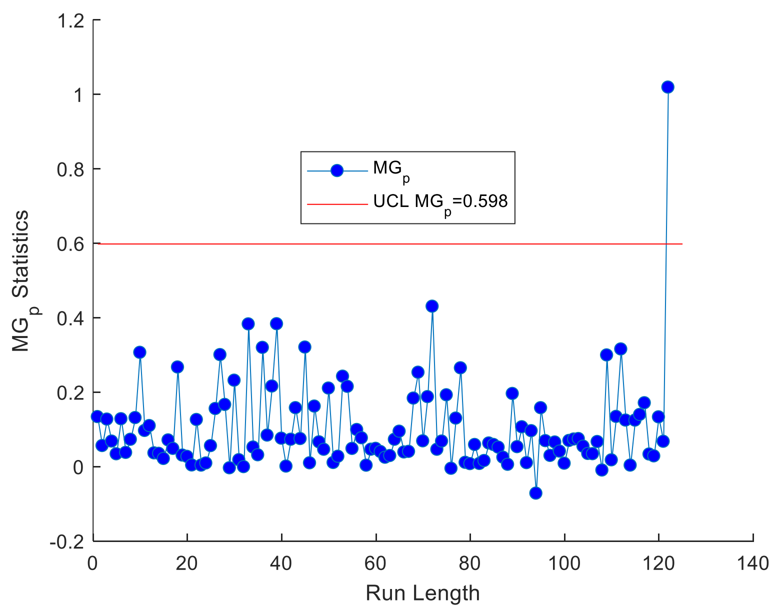

Fig 10. MG-*p* control chart under 0.2 $\sigma_{\hat{\varphi}}$ shift in φ

Figures 7 to 10 compare the performance of the MONS and MG-*p* control charts under the mentioned shifts in β_2 and φ. According to these figures, the signals received by the MONS and MG-*p* control charts occur at the 19th and 31th sample under -0.2 $\sigma_{\hat{\beta}_2}$ shift in β_2 and 106th and 122th sample under 0.2 $\sigma_{\hat{\varphi}}$ shift in φ, respectively. These results show that the MONS control chart detects the out-of-control condition faster than another chart under the mentioned shifts in β_2 and φ of the OLLM.

6- Conclusion and future research

In this paper, new MONS control chart was proposed to monitor the M-OLLM based processes in Phase II. The results obtained using simulation studies showed better performance of the MONS control chart in small and moderate shifts in all parameters of OLLM compared to the MG-*p* chart. In addition, some sensitivity analyses were done to evaluate the efficiency of the proposed control charts based on different values of smoothing parameters as well as different number of rows and columns of the OCT. The results showed that the proposed control char has better performance in detecting the out-of-control condition under $\lambda = 0.2$ in most individual shifts in M-OLLM parameters rather than the other smoothing parameters considered. Similar results are obtained under simultaneous shifts in the parameters of OLLM as well. Moreover, as the dimension of the contingency table increases, the performance of the proposed control chart improves. At the end, a real numerical example was applied to demonstrate the applicability of the proposed scheme and the results showed the superiority of MONS control chart rather than the MG-*p* chart in faster detection of the out-of-control condition. As a future research, monitoring the ordinal categorical processes in Phase I can be investigated. Moreover, modeling and monitoring the high dimensional ordinal contingency tables for both Phases I and II can be a suitable area for future research.

References

Agresti, A. (2003). *Categorical data analysis* (Vol. 482). John Wiley & Sons.

Agresti, A. (2010). *Analysis of ordinal categorical data* (Vol. 656). John Wiley & Sons.

Armitage, P. (1955). Tests for linear trends in proportions and frequencies. *Biometrics*, *11*(3), 375-386.

Beh, E.J., & Davy, P.J. (1998). Theory & Methods: Partitioning Pearson’s Chi-Squared Statistic for a Completely Ordered Three-Way Contingency Table. *Australian & New Zealand Journal of Statistics*, 40(4), 465-477.

Brzezińska, J. (2016). Ordinal Log-Linear Models for Contingency Tables. *Folia Oeconomica Stetinensia*, 16(1), 264-273.

Hakimi, A., Farughi, H., & Amiri, A. (2018). Phase II Monitoring of the Ordinal Multivariate Categorical Processes. *Submitted to Communications in Statistics-Simulation and Computation*.

Kamranrad, R., Amiri, A., & Niaki, S.T.A. (2017a). New Approaches in Monitoring Multivariate Categorical Processes based on Contingency Tables in Phase II. *Quality and Reliability Engineering International*, 33(5), 1105-1129.

Kamranrad, R., Amiri, A., & Niaki, S.T.A. (2017b). Phase II monitoring and diagnosing of multivariate categorical processes using generalized linear test-based control charts, *Communications in Statistics-Simulation and Computation*, 46(8), 5951-5980.

Kieffer, D., Bianchetti, L., & Poch, O. (2012). Wicker N. Perfect sampling on $2 \times \cdots \times 2 \times$ K contingency tables with an application to SAGE data. *Journal of Statistical Planning and Inference*, 142(4), 896-901.

Kijima, S., & Matsui, T. (2006). Polynomial time perfect sampling algorithm for two-rowed contingency tables. *Random Structures & Algorithms*, 29(2), 243-256.

Li, J., Tsung, F., & Zou, C. (2012). Directional control schemes for multivariate categorical processes. *Journal of Quality Technology*, 44(2), 136-154.

Li, Z., Zou, C., Wang, Z., & Huwang, L. (2013). A multivariate sign chart for monitoring process shape parameters. *Journal of Quality Technology,* 45(2), 149-165.

Li, J., Tsung, F., & Zou, C. (2014a). Multivariate binomial/multinomial control chart. *IIE Transactions,* 46(5), 526-542.

Li, J., Tsung, F., & Zou, C. (2014b). A simple categorical chart for detecting location shifts with ordinal information. *International Journal of Production Research,* 52(2), 550-562.

Lumley, T. (1996). Generalized estimating equations for ordinal data: A note on working correlation structures. *Biometrics,* 52(1), 354-361.

Subramanyam, K., & Rao M.B. (1989). Analysis of odds ratios in $2\times$n ordinal contingency tables. *Multivariate Statistics and Probability,* 27(1), 505-520.

Yashchin, E. (2012). On detection of changes in categorical data. *Quality Technology & Quantitative Management* 9(1),79-96.

Zafar, S., Cheema, S.A., Beh, E.J., Hudson, I.L., Hudson, S.A., & Abell, A.D. (2013). Linking ordinal log-linear models with Correspondence Analysis: an application to estimating drug-likeness in the drug discovery process. *20th International Congress on Modelling and Simulation, Adelaide, Australia,* 1941-1951.

Zhen, X., & Basawa, I.V. (2009). Categorical time series models for contingency tables. *Statistics & Probability Letters,* 79(10), 1331-1336.

Zou, C., & Tsung, F. (2011). A multivariate sign EWMA control chart. *Technometrics,* 53(1), 84-97.